



The kinetics and adsorption equilibrium of the removal of textile dyes from aqueous solutions by a bio-adsorbent produced from solid cassava (Manihot Esculenta Crantz) waste

Rafael Silva Dias

MSc., Federal University of Pará (Universidade Federal do Pará – UFPA), Brazil
diasrafael353@gmail.com

Lênio José Guerreiro de Faria

Doctor Professor, UFPA, Brazil.
leniojgfarria@gmail.com

Marlice Cruz Martelli

Doctor Professor, UFPA, Brasil.
martelli@ufpa.br

Davi do Socorro Barros Brasil

Doctor Professor, UFPA, Brazil.
dsbbrasil18@gmail.com

ABSTRACT

The chemical contamination of wastewater with textile dyes and the excessive generation of agro-industrial solid waste are the two issues addressed in this study. A possible solution to both problems is the production of activated carbon from solid cassava waste to remove the textile dyes, such as methylene blue, from wastewater. This study focused on the synthesis of activated carbon from cassava pulp for the adsorption of methylene blue. Therefore, the activated carbon precursor was characterized to analyze the total protein (0.51%), moisture (83.40%), oil (0%), and carbohydrate (16.10%) content. Kinetics and equilibrium tests were conducted using a fixed bed with 120 mg/L of dye and 0.01 g of carbon. The adsorption kinetics indicated a good fit to the intraparticle diffusion model, whereas the adsorption equilibrium sufficiently aligned with the Langmuir model. The activated carbon produced from the cassava pulp yielded highly satisfactory results under the experimental conditions evaluated in this study, thus may be used as an effective and low-cost bio-adsorbent to remove methylene blue dye from aqueous solutions. Accordingly, our study provides a potentially valuable solution to textile dye contamination and agro-industrial waste management problems while simultaneously utilizing a cassava by-product for beneficial and sustainable purposes.

KEYWORDS: Wastewater treatment. Adsorption. Pigments.

1 INTRODUCTION

Twice as much water is currently being consumed worldwide than it was two decades ago. Therefore, water is quickly becoming a scarce resource owing to its intensive use in agriculture, industry, households, and transportation combined with problems such as climate change (AHMED et al., 2021, p. 416). The chemical contamination of water is mostly caused by heavy metals, dyes, diluted organic solvents, pesticides, and herbicides, especially in industrial wastewater and groundwater (NORRAHIM et al., 2021, p. 7348).

Textile, paper, and leather industries discharge a high volume of wastewater contaminated with pigments into bodies of water (ARDILA-LEAL et al., 2021, p. 1). In particular, dye industries have expanded globally, producing nearly 8×10^5 tons of synthetic dyes annually (SLAMA et al., 2021, p. 2). In industrial wastewater, such components pose severe environmental problems owing to their toxicity to aquatic life and mutagenicity in humans (SINGH & ARORA, 2011, p. 809).

Concurrently, the industrial processing of cassava (*Manihot esculenta* Crantz) is also adversely affecting the environment. Naturally occurring in the Amazon region, cassava differs from other manioc varieties owing to its high moisture and low starch yield (SOUZA, 2010, p. 25). However, during processing for the extraction of manioc, several wastes are discarded, mainly solid wastes, such as outer (thin and brown) and inner (thick and white) peels, also known as bark and shavings, respectively, stumps, *crueira* [coarse cassava residue], fiber, bagasse, and byproducts, as well as liquid waste, such as washing water, press water, and starch processing water (MARTINEZ, 2017, p. 142).

In this regard, this study aims to optimize the conditions of activated carbon production from solid cassava waste, thereby utilizing this waste to prepare a bio-adsorbent for the removal of methylene blue to treat wastewater contaminated with this dye.

2 OBJECTIVES

The main objective of this study was to produce activated coal from cassava pulp as a bio-adsorbent to remove methylene blue dye in aqueous solutions. The specific aims were to characterize cassava pulp and to perform studies regarding activated coal adsorption kinetics and equilibrium.

3 METHODOLOGY

3.1 Raw material pretreatment

The roots were transferred in cloth bales to the Chemical Engineering Laboratory, where they were stored in refrigeration units. For the processing, the samples were washed before removing the peels. The remaining pulp was cut into small cubes and wrapped in filter material until being pressed by a Bovenau hydraulic press, which applied a 10-ton load to the sample. The resulting pressed disc was separated from the filter material and dried on a tray dryer with forced ventilation at 80°C for 24 h. The moisture content of the samples was simultaneously determined with the drying process. After 24 h, both the peel and the pulp components were removed from the dryer and crushed separately using a knife mill.

3.2 Total protein determination

A sample of the dried and ground pulp flour was collected to determine the total protein content using the modified Kjeldahl method, as well as the total amount of oils. The remaining samples from the crushing process were used to produce activated carbon. Equation 1 was applied to calculate the total protein content:

$$Protein (\%) = \frac{K * V * Factor}{P} \quad (1)$$

$K = Fc * 0.0014 * 100$

Fc = correction factor of a 0.1N sulfuric acid solution

P = sample mass in grams

V = volume of sulfuric acid solution used in the titration

Factor = nitrogen-to-protein conversion factor

3.3 Moisture determination

The total moisture was assessed by measuring 10 g of the sample before extracting the cassava juice in a tared metal capsule, and subsequently heating it for 3 h in a tray dryer. The sample was then cooled in a desiccator to room temperature before assessing the mass. The heating and cooling operation was repeated until a constant weight was obtained (LUTZ; LUTZ, 1985, p. 21). The collected data were applied in Equation 2:

$$\text{Moisture (\%)} = \frac{100 * N}{P} \quad (2)$$

N = Grams and moisture (Loss of mass in grams)

P = Sample mass

3.4 Determination of total oils

The total oil content was determined according to the Lutz and Lutz method (1985, p. 42). The total amount of oils was calculated using Equation 3.

$$\text{Oils}_{total}(\%) = \frac{100 * N}{P} \quad (3)$$

3.5 Determination of carbohydrates

The carbohydrate content of the samples was determined using the difference method, as shown in Equation 4 (OLIVEIRA JUNIOR, 2008, p. 2).

$$\text{Carbohydrates (\%)} = 100\% - (\text{Protein\%} + \text{Moisture\%} + \text{Oils}_{total}\%) \quad (4)$$

3.6 Activated carbon production.

Pre-dried cassava pulp was crushed in a knife mill. First, 100 g of material was chemically activated based on a modified version of the method by (KIM et al., 2001, p. 29), by wetting the precursor in 10.2% of H₂SO₄ and 97.59% Neon solutions at a ratio of 5:1. The mixture was maintained moistened for 24 h. Lastly, the material was washed with 2 liters of distilled water, after which the material was dried in an oven at 80 °C and then transferred to ceramic crucibles for pyrolysis in a muffle furnace at 600 °C for 3 h.

3.7 Standard calibration curve

The standard calibration curve of methylene blue was constructed by dissolving a stock solution to concentrations of 5, 10, 15, 20, 25, and 30 mg/L at a wavelength of 664 nm. The absorbance was determined on a Shimadzu UV-1800 spectrophotometer.

3.8 Adsorption kinetics and equilibrium

Adsorption kinetics and equilibrium studies were conducted using an aqueous solution of methylene blue as the adsorbate. The adsorption kinetics were analyzed by performing the experiment in a finite bath system, using a 125 mL Erlenmeyer flask with 100 mL of the contaminated solution and 0.04 g of activated carbon at room temperature (28°C). The samples

were obtained every 2 min for one hour, every 1 hour for the next 3 h, and then every 24 h after the first 4 h to measure the concentration of the contaminant in these samples. Different kinetics models were evaluated, namely the pseudo-first and pseudo-second order, intraparticle diffusion, and Elovich models. The equations used to fit the models to the experimental data are outlined in Table 1.

Table 1 – Adsorption kinetics models

Model	Equation
Pseudo-first order	$q_t = e^{1-Exp(-k*t)}$
Pseudo-second order	$q_t = \frac{(k_2 * q_e^2 * t)}{(1 + k_2 * q_e * t)}$
Intraparticle diffusion	$q_t = k * t^{0,5} + C$
Elovich	$q_t = \left(\frac{1}{\beta}\right) * \text{Log}(1 + A * B * t)$

Source: The authors, 2023.

Adsorption equilibrium tests were performed in a finite bath system at room temperature (28 °C) with 100 ml of the contaminated solution at varying initial concentrations (120, 100, 80, 60, and 40 mg/L), while maintaining the adsorbent mass at 0.04 g. Langmuir, Freundlich, and Redlich-Peterson isotherm models were tested for the adsorption equilibrium. The equations used to fit the models to the experimental data are outlined in Table 2.

Table 2 – Equilibrium isotherm models

Model	Equation
Langmuir	$q_e = q_{max} \left(\frac{b * C_e}{1 + b * C_e} \right)$
Freundlich	$q_e = K_f * (C_e)^{n_F}$
Redlich-Peterson	$q_e = \frac{K_{RP} * C_e}{1 + \alpha_{RP} * C_e^\beta}$

Source: The authors, 2023.

3.9 Chi-squared test (χ^2) and Coefficient of determination (R^2)

As shown in Equation 5, the Chi-squared test (χ^2) indicates the match between the observed (x_i) and calculated (y_i) frequencies, that is, the significant differences between the observed and calculated values are highlighted (Siegel; Castellan, 2008, p. 43).

$$\chi^2 = \sum_{i=k}^k \frac{(x_i - y_i)^2}{y_i} \quad (5)$$

The coefficient of determination (R^2) is the square of the Pearson product-moment correlation coefficient. According to Triola (1999, p. 235), two variables are correlated when one of them is positively related to the other to a certain extent.

The coefficient of determination expresses the proportion of variation in the dependent variable that is explained by the variation in the independent variable (Kennedy,

2008, p. 13). The mathematical relationship used to calculate the coefficient of determination is shown in Equation 6.

$$R^2 = \frac{(\sum(x_i - \bar{x})(y_i - \bar{y}))^2}{\sum(x_i - \bar{x})^2 \sum(y_i - \bar{y})^2} \quad (6)$$

RESULTS AND DISCUSSION

3.10 Total amount of protein, moisture, oils, and carbohydrates

The results of the total protein, moisture, oil, and carbohydrate contents are outlined in Table 3.

Table 3 – Results from the characterization of the raw material

Protein (%)	Moisture (%)	Oils total (%)	Carbohydrates (%)
0.51	83.40	0	16.10

Source: The authors, 2023.

3.11 Standard calibration curve

The results from the spectrophotometer readings used to construct the standard calibration curve are outlined in Table 4.

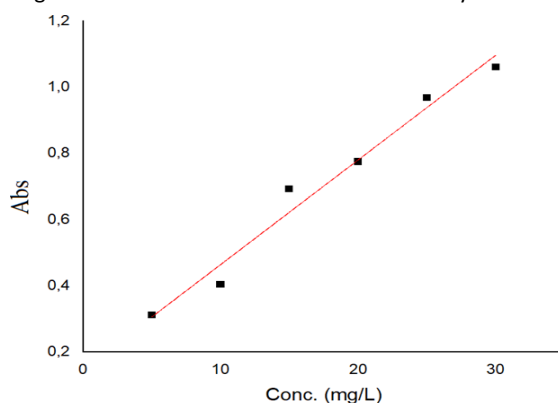
Table 4 – Absorbance results at specific concentrations

Sample	Concentration	ABS
01	5	0.164
02	10	0.252
03	15	0.531
04	20	0.748
05	25	0.885
06	30	1.003

Source: The authors, 2023.

Using this data, the standard calibration curve of the absorbance versus the concentration was constructed, as shown in Figure 1.

Figure 1 – Standard calibration curve of methylene blue



Source: The authors, 2023

The resulting equation of the curve (Equation 7) had an R^2 value of 0.9756.

$$y = 0.03608 x - 0.03427$$

(7)

3.12 Adsorption kinetics

The activated carbon adsorption kinetics was studied under the following conditions: 0.1 g of adsorbent (mass (m)), 100 mg L^{-1} of initial dye (concentration (C_0)), and 100 ml solution (volume (V)). The data outlined in Table 5 presents the amount of dye adsorbed per minute.

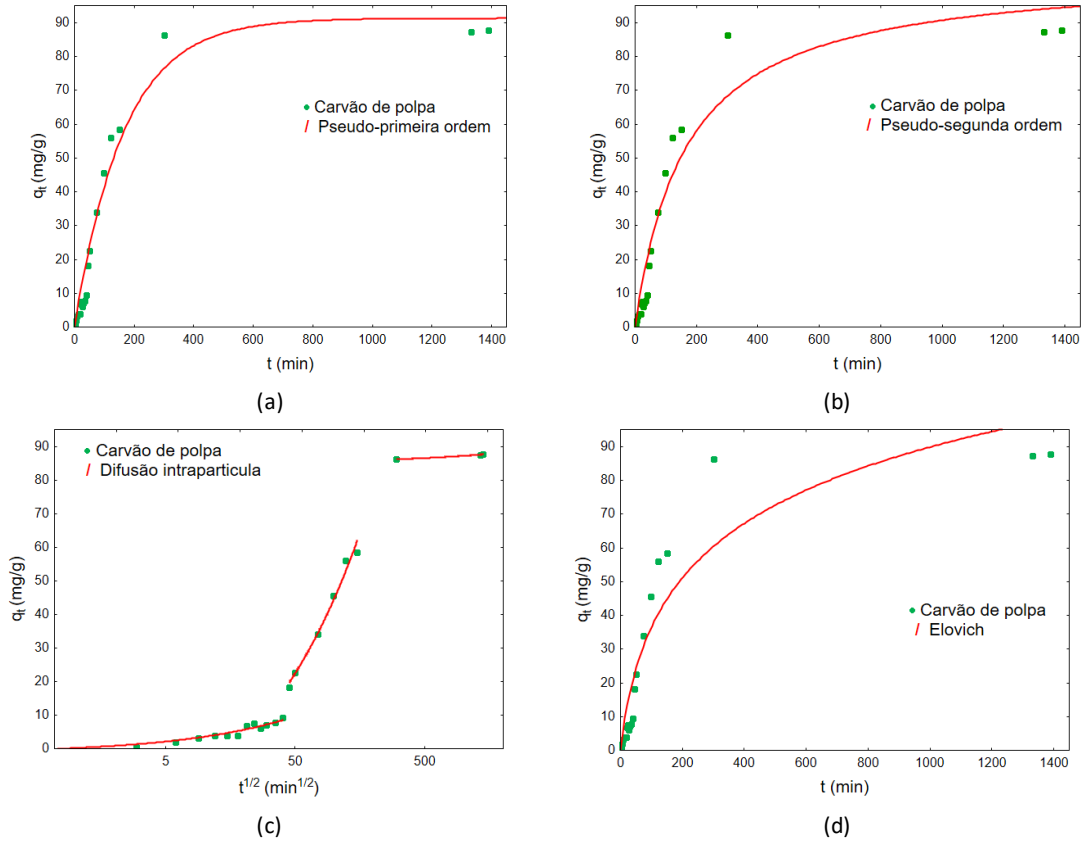
Table 5- Quantity of methylene blue adsorbed by the activated carbon at varying acquisition times.

t (min)	Q(mg/g)	t (min)	Q(mg/g)
0	0	35	7.8697
3	0.5372	40	9.3868
6	3.5000	45	18.2048
9	3.2553	50	22.6611
12	4.0139	60	34.0707
15	3.9190	64	45.5120
18	3.9190	88	55.9418
21	6.9216	112	58.4386
24	7.5221	150	86.1883
27	6.0366	1330	87.3577
30	7.0796	1390	87.8318

Source: The authors, 2023.

To analyze the adsorption kinetics, graphical curves were constructed to assess the variation in the amount of dye adsorbed by the activated coal as a function of time (Figure 2). The theoretical models were fitted to the experimental data in the Statistica software version 14 (USA), using the least squares loss function and the Levenberg-Marquard estimation method.

Figure 2 – Adsorption kinetics curves using (a) pseudo-first order, (b) pseudo-second order, (c) intraparticle diffusion and (d) Elovich models.

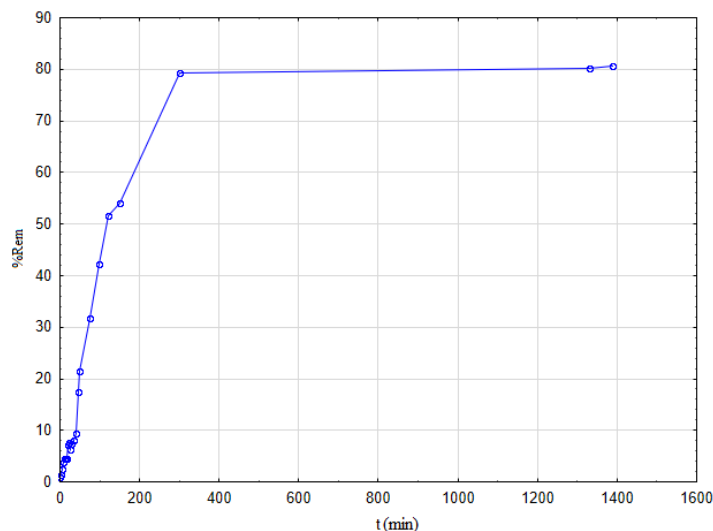


Source: The authors, 2023

The satisfactory convergence criterion was indicated by a difference in the loss function of lower than 1.0×10^{-6} for a maximum of 50 interactions.

The initial values of q_e and K_1 used to assess the convergence of the pseudo-first order (PPO) models were 100 and 0.00001, respectively. The Elovich equation converged with the initial conditions of B and A at 0.000001 and 10, respectively. The variation in the percentage of pulp removal over time is shown in Figure 3. The values were calculated by using Equation 8.

Figure 3 – Pulp removal percentage



Source: The authors, 2023

$$\%Rem = \left(\frac{q_i - q_f}{q_i} \right) * 100 \quad (8)$$

Figure 3 demonstrates that 80.71% of the contaminant dye was removed from the solution, which is nearly complete removal, indicating the high efficiency of the activated carbon adsorbent produced by using this process.

The calculated values of the parameters assessed by fitting the experimental curves are demonstrated in Table 6.

Table 6 – Parameters of the kinetics model

Models	Kinetic parameters			
	q _e	k ₁	R ²	X ²
PPO	91.28	0.006	0.98	661.47
PSO	q _e	k ₂	R ²	X ²
	105.61	0.00005	0.97	1209.61
Intraparticle diffusion	k _{df}	C	R ²	X ²
Stage I	1.56	-1.34	0.95	9.34
Stage II	7.61	-31.33	0.99	26.74
Stage III	0.07	84.92	0.97	0.09
Elovich	α	β	R ²	X ²
	0.80	0.04	0.94	2067.47

Source: The authors, 2023.

The results obtained from the adsorption kinetics study of cassava pulp-activated carbon demonstrated that the intraparticle diffusion model by Weber-Morris ($R^2=0.95; 0.99$ and 0.97) outperformed the other models assessed in this study, reaching the best χ^2 value in stage III. In every stage, $K_d1 < K_d2 > K_d3$, indicating that diffusion was slow in the first stage, which lasted 40 min, and accelerated in the next stage, when the dye adsorbed to a site on the internal or external surface of the activated carbon particles, with an energy depending on the coupling process (physical or chemical). Lastly, after 150 min, the adsorption rate decreased, with diffusion occurring in the adsorbate pores by the liquid-filled pores or by the diffusion mechanism in a solid medium (CHEUNG; SZETO; MCKAY, 2007, p. 2900). However, intraparticle diffusion was the only mechanism that controlled the adsorption across all the stages owing to non-zero linear coefficients (LEBRON; MOREIRA; SANTOS, 2019, p. 10; SILVA, 2015, p. 5).

The adsorption of methylene blue has been studied using different bio-adsorbents, including $Al_2(SO_4)_3$ -activated carbon produced from coconut, corn cobs, and banana peels. The adsorption kinetics study was conducted based on the pseudo-second order model. In the study performed by Yağmur and Kaya (2021, p. 7), the adsorption of methylene blue by coconut-activated carbon followed pseudo-second order kinetics, which demonstrated the following kinetic parameters: $K_2 = 1.66 \text{ g.mg}^{-1}.\text{min}^{-1}$ (adsorption rate constant) and $q_e = 21.23 \text{ g.mg}^{-1}$ (maximum adsorption). Furthermore, Medhat et al. (2021, p. 5) studied the adsorbents produced from corn cobs; however, their results also indicated pseudo-second order kinetics. For KOH-activated carbon, the kinetic parameters were $K_2 = 0.4 \text{ g.mg}^{-1}.\text{min}^{-1}$ and $q_e = 105.3 \text{ g.mg}^{-1}$. For $(NH_4)_2SO_4$ -activated adsorbents, the kinetic parameters were $K_2 = 3.7 \text{ g.mg}^{-1}.\text{min}^{-1}$ and $q_e = 85.5 \text{ g.mg}^{-1}$. Behling et al. (2017, p. 116) used $Al_2(SO_4)_3$ -activated carbon that was prepared from banana peels, in which pseudo-second order kinetics also proved adequate; the reported kinetic parameters were $K_2 = 30.9 \text{ g.mg}^{-1}.\text{min}^{-1}$ and $q_e = 13.44 \text{ mg.g}^{-1}$.

Cassava pulp-activated carbon cannot be compared with other models because this adsorbent does not have the same kinetic parameters. Regardless, its diffusion rate can be considered high, reaching concentrations near equilibrium in 150 min.

3.13 Adsorption equilibrium

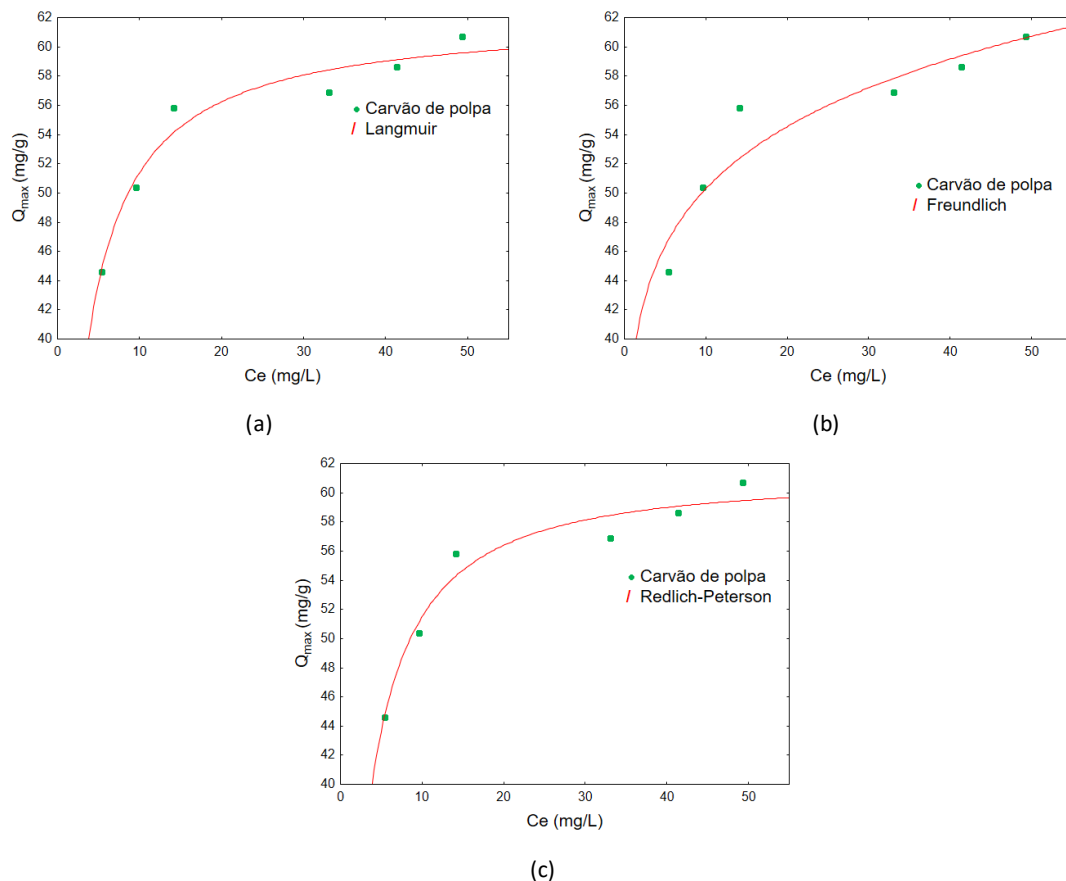
The experimental data from the adsorption isotherms of the cassava peel and pulp-activated carbon are outlined in Table 7. The conditions of the tool used to fit the model to the experimental data were the same as those used in the adsorption kinetics study. These values were used to produce the isotherms shown in Figure 4.

Table 7 – Concentration at equilibrium and the maximum amount adsorbed to activated carbon.

Ce (mg/L)	Qe (mg/g) pulp
5.388	44.612
9.607	50.393
14.158	55.842
33.106	56.894
41.371	58.629

Source: The authors, 2023.

Figure 4 – Adsorption isotherms fitted with the (a) Langmuir, (b) Freundlich, and (c) Redlich-Peterson models.



Source: The authors, 2023

The values of the isotherm parameters used to fit the models to the experimental data and their R^2 and χ^2 are outlined in Table 8.

Table 8 – Parameters of adsorption isotherm models

Models	Cassava pulp activated carbon				
	Langmuir	q_{max}	C_e	-	R^2
62.11		0.48	-	0.98	7.18
Freundlich	K_F	$1/n$	-	R^2	χ^2
	38.40	0.117	-	0.95	10.29
Redlich-Peterson	K_{RP}	α_{RP}	β	R^2	χ^2
	27.70	0.427	1.01	0.98	7.10

Source: Author, 2023.

The results from the analysis of the samples of activated carbon produced from cassava pulp demonstrated that the Langmuir and Redlich-Peterson models had the highest coefficients of determination and the lowest χ^2 values. Assuming monolayer adsorption on a homogeneous activated carbon surface, the Langmuir model enables a robust representation of the experimental data. Furthermore, by combining the characteristics of the Langmuir and

Freundlich isotherms, the Redlich-Peterson model is applicable to both homogeneous and heterogeneous systems and thus is highly versatile. The equilibrium adsorption capacity (q_e) has a linear relationship with the equilibrium concentration (C_e) in the numerator and an exponential relationship in the denominator. When the value of β is close to or 1, the Redlich-Peterson isotherm simplifies to the Langmuir isotherm, as shown in Table 8 (HU et al., 2021, p. 3; REDLICH; PETERSON, 2007, p. 1024). Additionally, the Freundlich model helps understand the affinity between the adsorbate and the adsorbent, with $K_F = 38.40 \text{ L.g}^{-1}$. The n parameters, ranging from 1 to 10, suggest a satisfactory degree of heterogeneity on the adsorption surface. In summary, these results indicate that the Langmuir isotherm prevails at low concentrations, whereas the Freundlich model appears to be more suitable for describing the adsorption at higher concentrations (YAĞMUR; KAYA, 2021, p. 9; ACOSTA et al., 2016 p. 173).

5. CONCLUSION

This study assessed the effects of temperature, acid concentration, and adsorbent contact time on the adsorption of methylene blue by cassava pulp-activated carbon. As demonstrated by characterizing the precursor, as well as measuring the total protein, moisture, oil, and carbohydrate contents, the experimental samples have typical characteristics of this cassava variety.

The maximum amount of adsorption at the equilibrium (Q_e) and percentage of removal (%Rem) were determined for 30 samples in the methylene blue adsorption tests, demonstrating that the characteristics of the activated carbon produced from Cassava pulp promoted the adsorption of the cationic dye, highlighting this adsorbent as a promising alternative for the utilization of cassava waste.

As shown by modeling the adsorption kinetics and equilibrium of the bio-adsorbent, the Weber-Morris intraparticle diffusion model best fitted the experimental data, indicating a high electrostatic affinity between the adsorbent and adsorbate. However, only the intraparticle diffusion model controlled the adsorption in all the stages owing to the non-zero linear coefficients. In the adsorption equilibrium study, the Langmuir isotherm demonstrated the best fit, indicating that adsorption occurred in a monolayer and that the activated carbon surface was homogeneous. The R_2 value of 0.98 indicates that the model explains 98% of the experimental variability.

6. Acknowledgements

The authors thank the National Council for Scientific and Technological Development (*Conselho Nacional de Desenvolvimento Científico e Tecnológico* – CNPq) for funding the project 2018 National Program for Academic Cooperation in the Amazon (*Programa Nacional de Cooperação Acadêmica na Amazônia* – PROCAD Amazônia 2018), Process: 88881.569753/2020-01 (Procad-AM)

REFERENCES

ACOSTA, R. et al. Tetracycline adsorption onto activated carbons produced by koh activation of tyre pyrolysis char. **Chemosphere**, v. 149, p. 168–176, 2016.

AHMED, S. et al. Recent developments in physical, biological, chemical, and hybrid treatment techniques for removing emerging contaminants from wastewater. **Journal of hazardous materials**, Elsevier, v. 416, p. 125912, 2021.

ARDILA-LEAL, Leidy D. et al. A brief history of colour, the environmental impact of synthetic dyes and removal by using laccases. **Molecules**, v. 26, n. 13, p. 3813, 2021.

BEHLING, S. M. *Produção de adsorvente carbonoso preparado a partir da ativação química e física de resíduos de casca de banana* [Production of activated carbon by chemical and physical activation of banana peel waste]. Tese (Doutorado) [Thesis (PhD)] - UFSC, Florianópolis, Rio Grande do Sul, Brasil, 2017.

CHEUNG, W.H. SZETO, Y.S. MCKAY, G. Intraparticle diffusion processes during acid dye adsorption onto chitosan. **Bioresource Technology**, v. 98, P. 2897-2904, Issue 15, 2007.

HU, Menghao, et al. Preparation of binder-less activated char briquettes from pyrolysis of sewage sludge for liquid-phase adsorption of methylene blue. **Journal of Environmental Management**, v. 299, p. 113601, 2021.

KENNEDY, Peter. **A Guide to Econometrics**. Massachusetts: Blackwell Publishing, 2008.

KIM, D.-Y. et al. High-yield carbonization of cellulose by sulfuric acid impregnation. **Cellulose**, Springer, v. 8, n. 1, p. 29–33, 2001.

LEBRON, Y.; MOREIRA, V.; SANTOS, L. Studies on dye biosorption enhancement by chemically modified fucus vesiculosus, spirulina maxima and chlorella pyrenoidosa algae. **Journal of Cleaner Production**, v. 240, p. 118197, 2019

INSTITUTO ADOLFO LUTZ. Normas Analíticas do Instituto Adolfo Lutz. v. 1: *Métodos químicos e físicos para análise de alimentos* [Chemical and physical methods for food analysis], 3. ed. São Paulo: IMESP, 1985. p. 21-43.

MARTINEZ, D. Potencial do resíduo do processamento da mandioca para produção de etanol de segunda geração [Potential of cassava processing waste for second-generation ethanol production]. **Revista Brasileira de Energias Renováveis**, v. 6, 2017.

MEDHAT, A. et al. Efficiently activated carbons from corn cob for methylene blue adsorption. **Applied Surface Science Advances**, v. 3, p. 100037, 2021.

NORRRAHIM, M. N. F. et al. Nanocellulose: A bioadsorbent for chemical contaminant remediation. **RSC advances**, p. 7347–7368, 2021.

OLIVEIRA JUNIOR, G. I. de, et al. *Composição centesimal de pericarpo de milho micropulverizado provenientes de processamento industrial* [Proximate composition of micro-pulverized corn pericarp from industrial processing]. **Belo Horizonte: Sociedade Brasileira de Ciência e Tecnologia de Alimentos**, 2008.

REDLICH, O.; PETERSON, D. A useful adsorption isotherm. **The Journal of Physical Chemistry**, v. 63, 2007.

SIEGEL, S.; CASTELLAN JR., J. *Estatística não-paramétrica para ciências do comportamento* [Nonparametric statistics for the behavioral sciences]. 2. ed. Porto Alegre: Bookman, 2008.

SILVA, T. et al. *Estudo cinético e de equilíbrio de adsorção para remoção de fenol em soluções aquosas utilizando carvão ativado com CO₂* [Adsorption kinetics and equilibrium study for phenol removal from aqueous solutions using activated carbon with CO₂]. **Blucher Chemical Engineering Proceedings**, n. 2, p. 6859–6866, 2015.



SINGH, Kamaljit; ARORA, Sucharita. Removal of synthetic textile dyes from wastewaters: a critical review on present treatment technologies. **Critical reviews in environmental science and technology**, n. 9, p. 807-878, 2011.

SLAMA, Houda Ben et al. Diversity of synthetic dyes from textile industries, discharge impacts and treatment methods. **Applied Sciences**, n. 14, p. 6255, 2021.

SOUZA, H. A. L. de. **Caracterização e Estudo da Viabilidade Tecnológica do Aproveitamento da Mandioca** [Characterization and Study of the Technological Feasibility of Cassava Utilization]. Tese (Doutorado em Engenharia de Alimentos) [Thesis (PhD in Food Engineering)] — Universidade Federal do Pará [Federal University of Pará], Belém, Belém, 2010.

TIBCO Software Inc., USA-Statistica 14.0, 2020.

TRIOLA, M. F. **Introdução à Estatística** [Introduction to Statistics]. Rio de Janeiro: LTC, 1999.

YAĞMUR, H. K.; KAYA İsmet. Synthesis and characterization of magnetic zncl₂-activated carbon produced from coconut shell for the adsorption of methylene blue. **Journal of Molecular Structure**, v. 1232, p. 130071, 2021.